

Multi-Resource Coordinate Scheduling for Earth Observation in Space Information Networks

Yu Wang, Min Sheng, *Senior Member, IEEE*, Weihua Zhuang, *Fellow, IEEE*,
 Shan Zhang, Ning Zhang, Runzi Liu, Jiandong Li, *Senior Member, IEEE*

Abstract—Space information network (SIN) is a promising networking architecture to significantly broaden the observation area and realize continuous information acquisition for Earth observation. Over the dynamic and complex SIN environment, it is a key issue to coordinate multi-dimensional heterogeneous network resources (e.g., observation resource and transmission resource) in the presence of multi-resource variations and severe conflicts, such that diverse Earth observation service requirements can be satisfied. To this end, this paper studies the multi-resource coordinate scheduling problem in SINs. Specifically, we first characterize the relationship among multi-resource using an event-driven time-expanded graph (EDTEG). Based on the EDTEG, observation resource and transmission resource are jointly considered, and an integer linear programming optimization problem is formulated to maximize the sum priorities of successfully scheduled tasks. An iterative optimization technique is employed to decompose the problem into separate observation scheduling and transmission scheduling sub-problems, which can be efficiently solved by extended transmission time sharing graph and directed acyclic graph methods, respectively. Simulation results demonstrate the effectiveness of the proposed algorithm and performance impacts of different network parameters.

Index Terms—Earth observation, space information networks, satellite networks, multi-resource coordination, scheduling, time-expanded graph, optimization, quality-of-service (QoS).

I. INTRODUCTION

Earth observation serves as a fundamental function in environment monitoring, intelligence reconnaissance, and natural disaster surveillance. Due to the inherent large coverage area, potential overflight ability and high survivability, Earth observation satellites (EOSs) are widely employed for diverse Earth observation missions. The EOSs typically operate in the sun-synchronous low-Earth orbits (LEOs) and acquire high-resolution image data with onboard sensors. Currently, different types of EOSs separately collect information and lack interactions among one another. This inevitably leads to under-utilization of scarce network resources [1]. Moreover, with the unprecedented growth of Earth observation traffic (e.g., 27.9 TB/day traffic on average for NASA Earth observing system [2]), traditional standalone EOS systems are unable to

accommodate such a huge amount of traffic and to provide satisfactory service guarantee. The problem is exaggerated especially in emergency situations, e.g., earthquakes, where EOSs are expected to rapidly react to user requests and continuously provide useful Earth observation data of concerning targets (e.g., certain observation area on the ground). The violent 8.0 magnitude earthquake that occurred in Wenchuan has demonstrated the insufficient service capability of Earth observation systems at that time [3].

To cater for the aforementioned issues, the concept of space information network (SIN) emerges [4]–[6]. A SIN is composed of heterogeneous EOS systems in different orbits that perform cooperative Earth observation, and geostationary-Earth orbit (GEO) relay satellites for timely observation data delivery between EOSs and destination ground stations. With the deployment of SINs, near-real-time data acquisition and transfer can be achieved [6]. However, the multi-dimensional heterogeneous resources (such as observation and transmission opportunities) are normally unbalanced and constrained in SINs. For example, a typical EOS can access a certain ground location for less than 10 minutes within the system period of approximately 100 minutes. This constraint gives EOSs limited chances to observe the targets of interest and to send all of their collected data to the destination. Therefore, how to design cooperative scheduling mechanisms and achieve efficient resource utilization to maximize the network utility becomes a key issue for SIN operation.

It is technically challenging to develop efficient multi-resource coordinate scheduling strategies for SINs, due to several reasons: 1) Because of the predictable but dynamic network connectivity, resource availability varies periodically and continuously. Moreover, there are various types of resources including observation, storage and transmission resources. It is difficult to precisely represent multi-dimensional resources in both time and space domains and characterize the correlation relationships among multiple heterogeneous resources; 2) There can be severe observation and transmission conflicts. On one hand, observation conflicts can occur frequently if the setup time between two successively observed targets in an EOS is not sufficient, and such conflicts vary in different EOSs. On the other hand, multi-resource limitations can lead to infeasibility of all potential observation and transmission opportunities, and thus induce observation and transmission conflicts [7]; 3) As different Earth observation tasks have diverse quality-of-service (QoS) requirements in terms of observation time duration and end-to-end delay, multi-resource scheduling should satisfy the differentiated service require-

This work is supported by the NSFC (No. 91638202 and 61725103), Key R&D Program – The Key Industry Innovation Chain of Shaanxi (No. 2017ZDCXL-GY-04-04). (Corresponding author: Min Sheng.)

Y. Wang, M. Sheng, R. Liu, and J. Li are with the State Key Laboratory of ISN, Xidian University, Xi'an 710071, China (e-mail: {yu_wang, rzliu}@stu.xidian.edu.cn; {msheng, jdli}@mail.xidian.edu.cn).

W. Zhuang, S. Zhang, and N. Zhang are with the Department of Electrical and Computer Engineering, University of Waterloo, Waterloo, ON N2L3G1, Canada (e-mail: {wzhuang, n35zhang}@uwaterloo.ca; zhang-shan11@mails.tsinghua.edu.cn).

ments in the dynamic and complex SIN environment.

In this paper, to address the technical challenges, we study the multi-dimensional resource scheduling problem for SINs. Specifically, an event-driven time-expanded graph (EDTEG) is employed to characterize multi-resource variations over the complex environment. Based on the EDTEG, a joint observation and transmission scheduling optimization framework is formulated, with the objective of maximizing the sum priorities of successfully scheduled tasks. Due to the NP-completeness of the optimization problem, an iterative optimization approach is proposed to decompose it into separate transmission scheduling sub-problem and observation scheduling sub-problem. For the transmission sub-problem, we utilize an extended time sharing graph to properly allocate transmission time among multiple EOSs. For the observation scheduling sub-problem, we use an acyclic directed graph to model the observation conflicts and a column generation method to solve the observation sub-problem, wherein the underlying generation problem is solved by multi-constrained optimal path based solutions. The two sub-problems are then updated iteratively by redistribution of surplus transmission time. The convergence of the proposed algorithm is proved and its computational complexity is analyzed in detail. Extensive simulation results are provided to demonstrate the performance gains of the proposed algorithm over existing benchmarks.

The main contributions of this paper are as follows:

- By exploiting an event-driven time-expanded graph, a joint optimization framework of observation and transmission scheduling is formulated to maximize the sum priorities of successfully scheduled observation tasks;
- An iterative optimization technique is utilized to decompose the problem into separate observation scheduling and transmission scheduling sub-problems, which are solved by acyclic directed graph and extended transmission time sharing graph, respectively;
- Extensive simulation results are provided to validate the effectiveness of our proposed scheduling algorithm. The effects of different network parameters on the network performance are evaluated.

The remainder of this paper is organized as follows. Section II gives an overview of related works. Section III introduces the SIN system model under consideration and gives the detailed problem formulation. We propose an approximate multi-resource scheduling algorithm in Section IV. The performance evaluation by simulations is presented in Section V, followed by concluding remarks and future research in Section VI.

II. RELATED WORKS

Resource scheduling plays a critical role in efficiently utilizing the network resources for SINs [8]–[10]. It can be classified into two main categories, namely single-resource scheduling and multi-resource coordinate scheduling.

Single-resource scheduling algorithms focus on scheduling only one type of network resources, i.e., observation resources or transmission resources. The observation resource scheduling is to allocate a subset of observation targets to multiple EOSs. Existing studies include static scheduling algorithms

for pre-planned targets and dynamic scheduling algorithms for real-time targets. The static observation scheduling problem has been investigated for both single-EOS [11], [12] and multiple-EOS [3], [13]. Various algorithms, including Lagrangian relaxation and graph techniques, are proposed to obtain an approximate solution. On the other hand, dynamic scheduling handles aperiodic observation targets whose arrival times are not known a priori. Under such a circumstance, rescheduling principles, e.g., backward shift and rehabilitation strategies [14] and target merging strategies [15], are developed to cope with random arrivals of new observation targets. In [16], an agent-based dynamic scheduling is presented to improve the global optimization and load balancing of observation resources. A comprehensive survey on observation scheduling solutions is given in [15].

The transmission scheduling problem focus on data exchange from EOSs to multiple destinations. In [17], the problem is investigated to resolve potential transmission conflicts, taking account of both the fairness requirement and overall transmission capacity. As an extension to [17], the data delivery time and resource usage are improved through making use of traffic information [18]. By considering the time-varying downlink channel quality, delay-optimal and throughput-optimal data downloading strategies are studied in [19] and [20], respectively. A throughput-optimal collaborative data downloading scheme is proposed to exploit data offloading opportunities between EOSs via inter-satellite links [21]. Besides, a two-phase dynamic task scheduling method for data relay satellites is proposed to complete the transmission tasks from each user satellite [22].

The existing single-resource scheduling algorithms result in low efficiency, if the observation and transmission resources are not properly matched. For instance, when an EOS scheduled to collect a large amount of observation data has a very short transmission time to a destination, the EOS is unable to download all its observation data to the destination. Therefore, each EOS should adjust the amount of data it collects during the observation scheduling process to match the data transmission time allocated in the transmission scheduling process, such that the network performance can be maximized.

Multi-resource coordinate scheduling algorithms schedule multiple types of resources simultaneously and balance the resources allocated in multiple phases, to provision satisfactory service in SINs. The joint observation and transmission scheduling problem for the COSMO-SkyMed constellation is first introduced in [23]. A heuristic scheme with look-ahead and back-tracking capabilities is then devised to produce feasible scheduling solutions. In [24], a constraint satisfaction optimization model is used to describe EOS observation tasks and data transmission jobs in an integrated way. Accordingly, a genetic algorithm based meta-heuristic is proposed. However, the transmission time sharing among multiple EOSs is neglected in the transmission scheduling procedure, which, to some extent, restricts the efficient utilization of transmission resources. We exploit an extended time-expanded graph method and propose an analytical framework to characterize multi-resource evolution over the complex SIN environment in [25]. The framework allows us to investigate the impact of dif-

ferent factors on the network performance, e.g., delay-limited throughput. Furthermore, a primal decomposition approach is presented in [26] to solve the optimization problem by taking advantage of its special structure. Although the proposed optimization framework and solution technique in [25], [26] are useful in deriving upper bounds of network throughput performance, they cannot capture the specific characteristics in terms of observation conflicts caused by insufficient setup time between multiple targets as well as non-preemptive observation time duration requirements. For a realistic SIN with a large number of targets, the computational complexity of the proposed algorithms is unacceptable.

To sum up, existing works either fail to model multi-resource evolution over SIN or incur high computational complexity. Most of them do not address the diverse service requirements of observation tasks, e.g., observation time duration and end-to-end delay. Different from these works, we study joint scheduling of observation resource and transmission resource to improve network performance, while considering SIN diverse requirements of multiple observation tasks.

III. SYSTEM MODEL AND PROBLEM FORMULATION

A. System Model

1) *Network Model*: Consider a SIN with three types of components: 1) a set $\mathcal{I} = \{1, \dots, I\}$ of I point targets (e.g., observation area) on the ground that need to be observed; 2) a set $\mathcal{K} = \{1, \dots, K\}$ of K EOSs moving in the LEOs to acquire observation data (e.g., high-resolution images) from the targets of interest and transmit the data to specified destinations; and 3) a set $\mathcal{N} = \{1, \dots, N\}$ of N destinations (i.e., relay satellites or ground stations) which serve as the sinks for all the observation data. The considered time horizon $\mathcal{T} = \{1, \dots, T\}$ is discretized into T time slots, each with a constant time duration τ . An example SIN with 2 targets, 2 EOSs and 1 destination relay satellite is depicted in Fig. 1(a).

There is a task, i , associated with each observation target, $i \in \mathcal{I}$. We use the terms target and task interchangeably when there is no ambiguity from context¹. All tasks are independent, non-preemptive and aperiodic [14]. New tasks normally arrive in a batch. Denote $\mathcal{I}_t \subset \mathcal{I}$ as the subset of tasks that arrive at the network at time slot t . A task, $i \in \mathcal{I}$, is described by a tuple comprised of four elements, i.e., $\{\mu_i, a_i, \rho_i, g_i\}$, where μ_i , a_i , ρ_i and g_i denote task i 's priority, arrival time slot, required continuous observation time duration, and expected finish time slot (i.e., the deadline when its observation data should be transmitted to destinations), respectively. Accurate information of all tasks is known a priori in time horizon \mathcal{T} .

There are three phases, namely observation phase, storage phase and transmission phase, to complete a task. Firstly, in the observation phase, an EOS is scheduled to collect observation data using its onboard imaging sensor (e.g., optical camera) when it is in the line-of-sight of the associated target. The time interval during which a target can be observed by an EOS is referred to as observation window (OW). Secondly, in the storage phase, an EOS stores the observation

data onboard and carry them forward until a transmission opportunity is available. Thirdly, in the transmission phase, an EOS downloads the data to a destination after it enters the coverage of the destination. The time interval when an EOS moves into the transmission range of a destination is termed as transmission window (TW). As shown in Fig. 1(a), EOS 1 first observes target 1 in the observation phase, stores the data in its buffer and carries them forward in the storage phase, and finally delivers the observation data to the destination in the transmission phase.

2) *Graph Model*: We herein use EDTEG² $\mathcal{G}^{\text{TEG}} = (\mathcal{V}^{\text{TEG}}, \mathcal{E}^{\text{TEG}})$ to model all the available OWs and TWs, where \mathcal{V}^{TEG} and \mathcal{E}^{TEG} represent the set of vertices and edges, respectively. The EDTEG is based on the predictable mobility trace [25] for the concerned SIN. We use the following steps to construct the EDTEG. Firstly, we build a unified two-dimensional time-space basis, wherein vertices correspond to targets, EOSs and destinations at different time slots. Secondly, edges denote the availability of different resources, i.e., OWs and TWs. If an edge exists, its corresponding resource is available and vice versa. Finally, we utilize a path formed by a set of contiguous vertices to capture the chronological relationship between observation phase and transmission phase. The detailed graph construction procedure is shown below.

i) **Vertices**: there are T layers in the constructed EDTEG, with each layer indicating network status at a single time slot. Within a time slot, the network is static, i.e., the status of an OW or a TW does not change. However, the network status may change during time slot transitions. At time slot t , target $i \in \mathcal{I}$, EOS $k \in \mathcal{K}$, and destination $n \in \mathcal{N}$ are represented by vertices o_i^t , s_k^t , and d_n^t in the EDTEG, respectively.

ii) **Edges**: there are three different types of directed edges in the EDTEG, namely observation edge, transmission edge and storage edge. Within a time slot, t , an observation edge (o_i^t, s_k^t) exists, if an observation opportunity³ is present between target i and EOS k during the time slot. Let $\mathcal{E}_t^{\text{ob}}$ denote the set of all observation edges in the graph at time slot t . Each observation edge, $(o_i^t, s_k^t) \in \mathcal{E}_t^{\text{ob}}$, is associated with a weight, $w(o_i^t, s_k^t)$, representing the amount of observation data volume acquired during time slot t . Similarly, a transmission edge (s_k^t, d_n^t) exists, if a transmission opportunity between EOS k and destination n is available during the time slot. Let $\mathcal{E}_t^{\text{tr}}$ denote the set of transmission edges in the graph at time slot t . Such type of transmission edge $(s_k^t, d_n^t) \in \mathcal{E}_t^{\text{tr}}$ is associated with a weight, $w(s_k^t, d_n^t)$, equal to the amount of data volume that can be delivered within the time slot. Let $w(s_k^t, d_n^t, i)$ denote the data volume delivered for target i on (s_k^t, d_n^t) , where $\sum_{i=1}^I w(s_k^t, d_n^t, i) = w(s_k^t, d_n^t)$ holds. On the other hand, during time slot transitions, a storage edge (s_k^t, s_k^{t+1}) is drawn to model that an EOS k can physically carry its data

²The motivation for EDTEG modeling is twofold. First, it facilitates multi-resource coordinate scheduling optimization problem formulation [27], [28]. Second, for a small-scale SIN, the optimal solution can be obtained to the optimization framework based on EDTEG [1]. It thus serves as a useful benchmark to evaluate the efficiency of proposed scheduling algorithms.

³An OW $[w^b, w^f]$ is generally represented by $(w^f - w^b + 1)$ continuous observation opportunities (i.e., observation edges) in the graph, where w^b and w^f denote the start time and ending time slots of the OW, respectively. Likewise, a TW is captured by several continuous transmission opportunities.

¹A target corresponds to an observation area on the ground. A task refers to both the observation and transmission phases of a target.

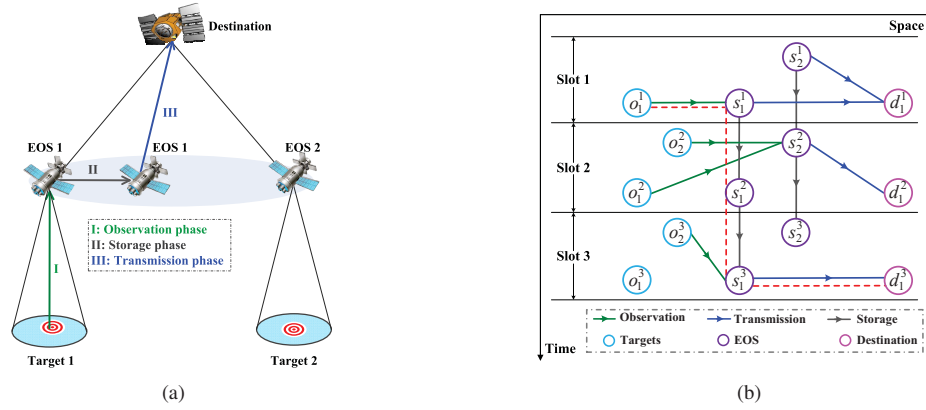


Figure 1. (a) An example SIN with 2 targets, 2 EOSs, and a destination relay satellite. Targets 1 and 2 arrive at the first and second time slots, respectively. (b) Corresponding EDTEG spanned over 3 time slots for the example SIN.

forward from time slot t to time slot $t + 1$. A storage edge is assumed to have a weight of infinity, i.e., $w(s_k^t, s_k^{t+1}) = \infty$, indicating that EOS k 's onboard buffer size is infinite.

iii) Paths: a path is a sequence of distinct vertices in the directed graph. It originates from a vertex representing the target and ends at a vertex representing the destination. The set of edges that it traverses can thus capture the sequentially chained multi-dimensional resources (i.e., OWs and TWs). An example of its derivation is given in Fig. 1(b). The time horizon is set to 3 time slots. There are 3 vertices created for an EOS or a destination, but only two vertices, i.e., $\{o_2^2, o_2^3\}$, for target 2. This is because vertices corresponding to target 2 are created only upon its arrival. As indicated by observation edge (o_2^2, s_2^2) , target 2 can be observed by EOS 2 at time slot 2. Similarly, with transmission edge (s_1^3, d_1^3) , a transmission opportunity exists between EOS 1 and the destination at time slot 3. The path, $\{o_1^1, s_1^1, s_1^2, s_1^3, d_1^3\}$, represented by the red dotted line in the graph, indicates that EOS 1 can observe target 1 at time slot 1, carry the observation data at time slot 2, and then transmit them to the destination at time slot 3.

B. Problem Formulation

1) Basic Constraints: Herein, we formulate some basic constraints on the constructed EDTEG. To be specific, the observation and transmission constraints are introduced for observation and transmission phases, respectively. Meanwhile, the interactions between the two phases are characterized by flow conservation constraints. Note that we neglect the storage constraints herein based on the assumption that each EOS is equipped with infinite buffer.

Observation constraints. Define an observation scheduling vector $\mathbf{X} = \{x(o_i^t, s_k^t) | t \in \mathcal{T}, (o_i^t, s_k^t) \in \mathcal{E}_t^{\text{ob}}\}$ to reflect the mapping of I targets to K EOSs, where the binary element $x(o_i^t, s_k^t) = 1$ if target i is observed by EOS k at time slot t , and $x(o_i^t, s_k^t) = 0$ otherwise. Considering that an EOS can process at most one target at a time slot, we have

$$\sum_{o_i^t: (o_i^t, s_k^t) \in \mathcal{E}_t^{\text{ob}}} x(o_i^t, s_k^t) \leq 1, \quad \forall k, t. \quad (1)$$

Meanwhile, if target i is observed, its non-preemptive observation duration requirement should be satisfied, which yields

$$\sum_{t=b_{i,k}}^{f_{i,k}} \sum_{s_k^t: (o_i^t, s_k^t) \in \mathcal{E}_t^{\text{ob}}} x(o_i^t, s_k^t) = \rho_i, \quad \forall i \quad (2)$$

where $b_{i,k}$ and $f_{i,k}$ denote the observation beginning time and ending time of target i by EOS k , respectively, and $f_{i,k} = b_{i,k} + \rho_i$ holds. According to [23], [29], both $b_{i,k}$ and $f_{i,k}$ can be predetermined, because they depend on the flight parameters of EOS k . Note that (2) implies that, from time slot $b_{i,k}$, contiguous ρ_i time slots within available OWs in EOS k are allocated together to complete observation of target i .

When a target is observed, an EOS requires a setup time to maneuver its position or sensor orientation [12]. To capture this sequence-dependent feature, we further define a vector, $\mathbf{Z} = \{z_{i,j}\}$, where binary variable $z_{i,j} = 1$ if target j is observed after target i by the same EOS, and $z_{i,j} = 0$ otherwise. Since there should be sufficient setup time to observe successive targets in an EOS, we have

$$f_{i,k} + \delta_{i,j,k} \leq b_{j,k} + (1 - z_{i,j})H, \quad \forall i, j, k \quad (3)$$

where H is a sufficiently large positive constant, and $\delta_{i,j,k}$ is the setup time from executing target i to target j by EOS k .

Transmission constraints. Due to limited resources (e.g., transponders) in EOSs, only a subset of potential transmission opportunities within TWs can be utilized for data transmission [30]. To this end, we define a transmission scheduling vector, $\mathbf{Y} = \{y(s_k^t, d_n^t) | t \in \mathcal{T}, (s_k^t, d_n^t) \in \mathcal{E}_t^{\text{tr}}\}$, where $y(s_k^t, d_n^t) = 1$ if EOS k is scheduled to transmit to destination n at time slot t , and $y(s_k^t, d_n^t) = 0$ otherwise. Following [26], we assume that a destination can support one transmission at a time slot. In addition, an EOS can transmit to a destination at a time slot. Thus, the following constraints should be satisfied,

$$\sum_{s_k^t: (s_k^t, d_n^t) \in \mathcal{E}_t^{\text{tr}}} y(s_k^t, d_n^t) \leq 1, \quad \forall n, t \quad (4)$$

$$\sum_{d_n^t: (s_k^t, d_n^t) \in \mathcal{E}_t^{\text{tr}}} y(s_k^t, d_n^t) \leq 1, \quad \forall k, t. \quad (5)$$

Flow conservation constraints. The total amount of data transmitted by EOS k to destinations must not exceed the amount of data that it acquired, by the end of time slot t ($t \in \{1, \dots, T - 1\}$). That is,

$$\sum_{t=1}^{\theta} \sum_{o_i^t: (o_i^t, s_k^t) \in \mathcal{E}_t^{\text{ob}}} w(o_i^t, s_k^t) - \sum_{t=1}^{\theta} \sum_{d_n^t: (s_k^t, d_n^t) \in \mathcal{E}_t^{\text{tr}}} w(s_k^t, d_n^t) \geq 0, \quad \forall \theta \in \{1, \dots, T-1\}, k \quad (6)$$

where the first item and second item correspond to the total data observed and transmitted during θ time slots, respectively. Note that the inequality permits the EOS to hold data and carry them forward into future time slots [31]. Besides, in (6), $w(o_i^t, s_k^t)$ and $w(s_k^t, d_n^t)$ should satisfy

$$w(o_i^t, s_k^t) = x(o_i^t, s_k^t) \cdot r_k^{\text{ob}} \cdot \tau, \quad \forall t, (o_i^t, s_k^t) \in \mathcal{E}_t^{\text{ob}} \quad (7)$$

$$w(s_k^t, d_n^t) = y(s_k^t, d_n^t) \cdot r_k^{\text{tr}} \cdot \tau, \quad \forall t, (s_k^t, d_n^t) \in \mathcal{E}_t^{\text{tr}} \quad (8)$$

where r_k^{ob} and r_k^{tr} represent the data collection rate and data transmission capacity for EOS k , respectively.

Finally, we impose that the total observation data volume for a scheduled task should equal to that delivered to destinations before its expected finish time, which is

$$\sum_{t=a_i}^{g_i} \sum_{s_k^t: (o_i^t, s_k^t) \in \mathcal{E}_t^{\text{ob}}} w(o_i^t, s_k^t) = \sum_{t=a_i}^{g_i} \sum_{(s_k^t, d_n^t) \in \mathcal{E}_t^{\text{tr}}} w(s_k^t, d_n^t, i), \quad \forall i. \quad (9)$$

2) *Optimization Problem Formulation:* Given the constructed EDTEG, the problem under consideration is to select and schedule a subset of targets to different OWs, while considering the transmission scheduling of multiple TWs. Our objective is to maximize the sum priorities of successfully scheduled tasks. A task is successfully scheduled if and only if its associated target is observed and the required observation data are transmitted to destinations before the expected finish time. We formulate it as the optimization problem (P1):

$$\begin{aligned} (\text{P1}) \quad & \max_{\mathbf{x}, \mathbf{y}, \mathbf{z}} \sum_{t \in T} \sum_{(o_i^t, s_k^t) \in \mathcal{E}_t^{\text{ob}}} \frac{\mu_i}{\rho_i} x(o_i^t, s_k^t) \\ \text{s.t.} \quad & (1) - (9). \end{aligned} \quad (10)$$

In problem (P1), the objective is to maximize the total successfully scheduled tasks weighted by their priorities, subject to observation constraints (1)-(3), transmission constraints (4)-(5), and flow conservation constraints (6)-(9). Notice that the coefficient $\frac{\mu_i}{\rho_i}$ in the objective function stands for the average priority received from one time slot observation. Observe that problem (P1) is an integer linear programming (ILP) problem, since both the objective and constraints are linear functions, and it only involves integer decision variables.

Lemma 1. *Problem (P1) is NP-complete to solve.*

Proof: Consider a generalized case where all the transmission constraints (4)-(5) and flow conservation constraints (6)-(9) are relaxed. In this case, problem (P1) is reduced to the satellite range scheduling problem with non-identical machines, which is already an NP-complete problem. Accordingly, the original problem (P1) is NP-complete to solve. ■

In addition to its NP-completeness, there are some other aspects that increase the computational complexity of solving the

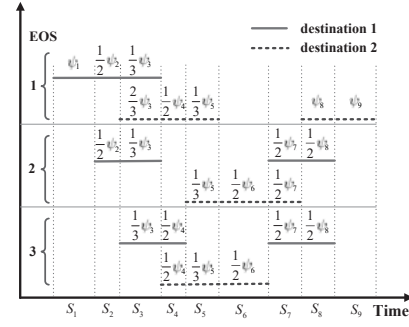


Figure 2. An example of extended transmission time sharing graph with 3 EOSs and 2 destinations. The whole time horizon includes 9 segments. An initial allocation of transmission time is labeled on the segments.

multi-resource scheduling problem (P1). The observation and transmission constraints are tightly coupled by the flow conservation constraints. It is challenging to directly decompose such couplings. On one hand, as indicated by (6), the coupling relationship is time dependent and spans nearly over the entire time horizon; on the other hand, because both the observation and transmission scheduling problems involve integer decision variables, it will inevitably lead to non-negligible optimality gap if traditional decomposing techniques, e.g., Lagrangian decomposition technique, are used [32].

For a small-scale SIN, existing optimization toolkits can provide an optimal solution to the optimization problem based on EDTEG [1]. However, for a large-scale SIN, it is computationally prohibitive to directly employ existing algorithms without taking the specific structure of problem (P1) into consideration. This is because building the EDTEG alone with a large number of targets over long time horizon incurs extremely high complexity [26]. On the other hand, the scheduling problem is an oversubscribed problem and involves a large number of decision variables [33]. In view of these, we aim to devise an approximate scheduling algorithm to reduce complexity in solving the optimization problem.

IV. APPROXIMATE MULTI-RESOURCE SCHEDULE

In this section, we propose an approximate multi-resource scheduling (AMRS) algorithm to solve problem (P1). In AMRS algorithm, the original problem (P1) is decomposed into a transmission scheduling sub-problem and an observation scheduling sub-problem. Then, an iterative optimization method is utilized to asymptotically reach the desired solution. The transmission scheduling sub-problem is solved by exploiting an extended transmission time sharing graph method. The observation scheduling sub-problem is tackled by the column generation approach, wherein the underlying generation problem is determined by finding multi-constrained optimal paths on a constructed acyclic directed graph (ADG). The above two sub-problems are updated iteratively through a procedure of redistributing surplus transmission time.

A. Transmission Scheduling Sub-problem

We employ an extended transmission time sharing graph method [21] to deal with the transmission scheduling between multiple EOSs and destinations (i.e., multiple TWs). The

extended transmission time sharing graph is constructed as follows. As shown in Fig. 2, the time horizon is divided by the start-times and end-times of all potential TWs. Two adjacent time points on the time horizon form a segment, denoted by S_m ($m = 1, 2, \dots, M$). Let ς_m^b and ς_m^f be the beginning time and ending time of segment S_m . The time duration, ψ_m , of segment S_m can be expressed as $\psi_m = \varsigma_m^f - \varsigma_m^b$. The total time duration ψ_m is shared among EOSs at the same destination over segment S_m . As depicted in Fig. 2, segment S_3 for destination 1 is shared by EOS 1, EOS 3 and EOS 4. For an EOS, if TWs for different destinations overlap at a segment, transmission time over the segment should also be properly shared. For instance, transmission time of EOS 1 over segment S_3 is distributed between destinations 1 and 2.

Define $\mathcal{C} = \{(c_{1,1}^1, c_{1,2}^1, \dots, c_{k,n}^m, \dots, c_{K,N}^M)\}$ as a multidimensional capacity region of all the transmission time combinations that multiple TWs can support for data transmission, where $c_{k,n}^m$ denotes the amount of allocated transmission time in segment S_m between EOS k and destination n . We use the following lemma to characterize \mathcal{C} .

Lemma 2. Capacity region \mathcal{C} is constituted by the set of transmission time $(c_{1,1}^1, c_{1,2}^1, \dots, c_{K,N}^M)$ such that

$$\sum_{k \in \mathcal{K}} c_{k,n}^m \leq \psi_m, \quad \forall m, n \quad (11)$$

$$\sum_{n \in \mathcal{N}} c_{k,n}^m \leq \psi_m, \quad \forall m, k. \quad (12)$$

Proof: Capacity region \mathcal{C} should be bounded by the following two conditions: 1) For destination n , the allocated transmission time to all EOSs sharing segment S_m should not exceed the maximum available transmission time, i.e., ψ_m , represented by (11); 2) The sum transmission time from EOS k to all destinations over segment S_m is less than ψ_m , represented by (12). Putting (11) and (12) together, we can obtain capacity region \mathcal{C} . ■

Observe that (4) and (5) can be captured by (11) and (12), respectively. As the initial allocation of transmission scheduling between EOSs and destinations, we equally distribute the transmission time among the EOSs that share the segment for the same destination. It can be observed that segment S_2 is shared by EOS 1 and EOS 2 at destination 1, so the transmission time allocated to each EOS is $\frac{1}{2}\psi_2$, i.e., $c_{1,1}^2 = c_{2,1}^2 = \frac{1}{2}\psi_2$. For an EOS, the total available transmission time over a segment for different destinations should not exceed the length of the segment. As can be seen from Fig. 2, the allocated transmission time over segment S_3 for EOS 1 at destination 2 is $\frac{2}{3}\psi_3$, i.e., $c_{1,2}^3 = \frac{2}{3}\psi_3$, because the rest time is already given to destination 1 with $c_{1,1}^3 = \frac{1}{3}\psi_3$. Let $D_{k,m}^t$ denote the actual transmission time allocated to EOS k in segment S_m . The sum of transmission time, D_k^t , allocated to EOS k in all segments during the whole time horizon is $D_k^t = \sum_m \sum_n c_{k,n}^m = \sum_m D_{k,m}^t$. For example, the total TWs for EOS 2 comprise six segments, S_2, S_3, S_5, S_6, S_7 and S_8 . Segments S_2, S_3, S_5, S_6 and S_8 are shared by 2, 3, 3, 2 and 2 EOSs, respectively, while segment S_7 is shared by transmissions at both destinations. Consequently, we have $D_2^t = \frac{1}{2}\psi_2 + \frac{1}{3}\psi_3 + \frac{1}{3}\psi_5 + \frac{1}{2}\psi_6 + \psi_7 + \frac{1}{2}\psi_8$.

B. Observation Scheduling Sub-problem

Given an allocated transmission time vector $(D_{1,1}^t, D_{1,2}^t, \dots, D_{K,M}^t)$, we need to deal with the observation scheduling sub-problem, i.e., schedule a subset of observation targets for each EOS. Specifically, we first reformulate the optimization problem (P1) based on ADG, which can capture all the possible observation sequences. After that, we employ the column generation method to solve the problem on the constructed graph with low complexity.

1) *Problem Transformation with ADG*: The original problem (P1) reduces to the following optimization problem (P2):

$$\begin{aligned} (\text{P2}) \quad & \max_{\mathbf{X}, \mathbf{Z}} \sum_{t \in \mathcal{T}} \sum_{(o_i^t, s_k^t) \in \mathcal{E}_t^{\text{ob}}} \frac{\mu_i}{\rho_i} x(o_i^t, s_k^t) \\ \text{s.t.} \quad & (1)-(3), (7), (9) \\ & \sum_{t=1}^{\theta} \sum_{o_j^t: (o_j^t, s_k^t) \in \mathcal{E}_t^{\text{ob}}} w(o_j^t, s_k^t) \geq F_{k,t}^t, \\ & \quad \forall \theta \in \{1, \dots, T-1\}, k \end{aligned} \quad (13)$$

where $F_{k,t}^t$ is the allocated transmission time to EOS k before time slot t . Noticeably, given $(D_{1,1}^t, D_{1,2}^t, \dots, D_{K,M}^t)$, $F_{k,t}^t$ can be approximately obtained by

$$F_{k,t}^t = \sum_{m: \varsigma_m^b \leq t < \varsigma_{m+1}^b} D_{k,m}^t + \frac{t - \varsigma_m^b}{\psi_{m+1}} \cdot D_{k,m+1}^t, \quad \forall k, t \quad (14)$$

where $\frac{t - \varsigma_m^b}{\psi_{m+1}}$ represents the proportion of considered time duration $(t - \varsigma_m^b)$ in segment S_{m+1} . Compared with problem (P1), transmission constraints (4) and (5) are removed in problem (P2). Also, (6) and (8) are represented by (13) in problem (P2). Problem (P2) can be reformulated and solved based on the definition of observation sequence.

Definition 1. An observation sequence $\ell = \{\dots, o_i, o_j, \dots\}$ is a set of ordered targets that can be sequentially observed by an EOS, with any two adjacent elements, (o_i, o_j) , satisfying

$$b_{i,k} + \rho_i + \delta_{i,j,k} \leq b_{j,k}, \quad \forall (o_i, o_j). \quad (15)$$

Note that (15) can replace (3). Let $\mathcal{L} = \{\mathcal{L}_1 \cup \mathcal{L}_2 \dots \cup \mathcal{L}_K\}$, where \mathcal{L}_k represents all the feasible options for observation sequences on EOS k . The set of all possible observation sequences for EOS k is obtained using an ADG $\mathcal{G}_k^{\text{ADG}} = (\mathcal{V}_k^{\text{ADG}}, \mathcal{E}_k^{\text{ADG}})$ [29], where $\mathcal{V}_k^{\text{ADG}}$ and $\mathcal{E}_k^{\text{ADG}}$ are the set of vertices and edges, respectively. If target i can be observed by EOS k , a vertex $o_i \in \mathcal{V}_k^{\text{ADG}}$ is created in $\mathcal{G}_k^{\text{ADG}}$. If two targets i and j can be observed successively by EOS k (i.e., the setup time constraint (3) holds), a directed edge $(o_i, o_j) \in \mathcal{E}_k^{\text{ADG}}$ exists. We add two virtual vertices v_s and v_d to represent the common source and destination in $\mathcal{G}_k^{\text{ADG}}$, respectively. A path from v_s to v_d in the graph thus corresponds to an observation sequence. An example ADG is given in Fig. 3. There is an observation conflict between targets 1 and 2, since edge (o_1, o_2) does not exist in the graph. Meanwhile, the example path $\{v_s, o_1, o_3, o_4, v_d\}$ corresponding to $\ell = \{o_1, o_3, o_4\}$ indicates that the EOS can observe targets 1, 3, and 4 successively.

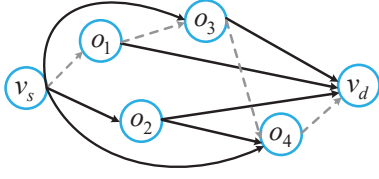


Figure 3. An example of directed acyclic graph.

Based on the preceding notations, we can reformulate the optimization problem (P2). The sum priority, f_ℓ^k , of observation sequence ℓ for EOS k becomes $f_\ell^k = \sum_{i \in \mathcal{I}} \mu_i \nu_{i,\ell}^k$, where $\nu_{i,\ell}^k = 1$ if observation sequence ℓ of EOS k contains target i , and $\nu_{i,\ell}^k = 0$ otherwise. Thus, the following equation holds,

$$\sum_{t \in \mathcal{T}} \sum_{(o_i^t, s_k^t) \in \mathcal{E}_t^{\text{ob}}} \frac{\mu_i}{\rho_i} x(o_i^t, s_k^t) = \sum_{k \in \mathcal{K}} \sum_{\ell \in \mathcal{L}_k} a_\ell^k f_\ell^k \quad (16)$$

where $a_\ell^k = 1$ if observation sequence ℓ is assigned to EOS k , and $a_\ell^k = 0$ otherwise. Define $\mathbf{A} = \{a_\ell^k\}$ as the assignment vector. Problem (P2) is equivalent to problem (P3), given by

$$\begin{aligned} (\text{P3}) \quad & \max_{\mathbf{A}} \sum_{k \in \mathcal{K}} \sum_{\ell \in \mathcal{L}_k} a_\ell^k f_\ell^k \\ \text{s.t.} \quad & \sum_{k \in \mathcal{K}} \sum_{\ell \in \mathcal{L}_k} a_\ell^k \nu_{i,\ell}^k \leq 1, \quad \forall i \\ & \sum_{\ell \in \mathcal{L}_k} a_\ell^k \leq 1, \quad \forall k \end{aligned} \quad (17)$$

$$\sum_{\ell \in \mathcal{L}_k} a_\ell^k \leq 1, \quad \forall k \quad (18)$$

$$a_\ell^k \in \{0, 1\}, \quad \forall \ell, k \quad (19)$$

$$\sum_{i: g_i > \zeta_m^f} \rho_i \cdot \nu_{i,\ell}^k \cdot r_k^{\text{ob}} \leq \sum_{\vartheta=1}^m D_{k,\vartheta}^{\text{tr}} \cdot r_k^{\text{tr}}, \quad \forall m \in \{1, \dots, M\}, k \quad (20)$$

where (17) allows each task to be processed by an EOS at most once, (18) ensures that each EOS should have only one assignment in the final optimal solution, and (20) states that obtained data volume for scheduled tasks with finish time more than ζ_m^f in EOS k should be transmitted to destinations timely. (20) replaces (9) and (10) in problem (P2).

2) *Column Generation Solution Method*: As the number of targets increases, listing all observation sequences, \mathcal{L} , in constructed ADGs is not scalable because the number of observation sequences grow exponentially with the number of targets. To circumvent this difficulty, the column generation (CG) method [34], [35] is employed. For problem (P3), CG approach decomposes (P3) into a master problem (P3-M) and a set of K generation problems (P3-G), one for each EOS. The problems (P3-M) and (P3-G) are solved iteratively until an optimal criteria is met. Master problem (P3-M) is initialized with a selected subset of observation sequences $\mathcal{L}_0 = \{\mathcal{L}'_1 \cup \mathcal{L}'_2 \dots \cup \mathcal{L}'_K\}$, that satisfy all constraints in (P3). Since the number of observation sequences, $|\mathcal{L}_0|$, in master problem (P3-M) is much smaller than that, $|\mathcal{L}|$, of the original problem (P3), the complexity in solving master problem (P3-M) is significantly reduced. In generation problem (P3-G), we use duality theory to verify the optimality of master problem (P3-M). Then, a set of new observation sequences is selected and added to master problem (P3-M) to improve the results.

The master problem, (P3-M), for EOS k is formulated as

$$\begin{aligned} (\text{P3-M}) \quad & \max_{\mathbf{A}} \sum_{k \in \mathcal{K}} \sum_{\ell \in \mathcal{L}'_k} a_\ell^k f_\ell^k \\ \text{s.t.} \quad & \sum_{k \in \mathcal{K}} \sum_{\ell \in \mathcal{L}'_k} a_\ell^k \nu_{i,\ell}^k \leq 1, \quad \forall i \end{aligned} \quad (21)$$

$$\sum_{\ell \in \mathcal{L}'_k} a_\ell^k \leq 1, \quad \forall k \quad (22)$$

$$a_\ell^k \in \{0, 1\}, \quad \forall \ell. \quad (23)$$

A lemma is given to show the property of problem (P3-M).

Lemma 3. *Problem (P3-M) is a weighted set packing problem.*

Proof: First, we show that (22) can be removed in problem (P3-M) without affecting its optimality by contradiction. Assume that there exists an EOS, k , satisfying $\sum_{\ell \in \mathcal{L}'_k} a_\ell^k > 1$. Accordingly, at least two observation sequences, e.g., ℓ_1 and ℓ_2 , are selected for the EOS, i.e., $a_{\ell_1}^k = a_{\ell_2}^k = 1$. If both ℓ_1 and ℓ_2 contain the same target i , we derive $\sum_{\ell \in \mathcal{L}'_k} a_\ell^k \nu_{i,\ell}^k > 1$. Clearly, (21) is violated. Otherwise, we can equivalently substitute a new observation sequence $\ell = \{\ell_1 \cup \ell_2\}$. Thus, problem (P3) can be reformulated by removing (22), wherein an observation sequence ℓ corresponds to a set, and f_ℓ^k is its weight. To this end, it can be seen that problem (P3-M) turns into a weighted set packing problem [36]. ■

Problem (P3-M) can be approximately solved by local search algorithms [36], [37] or simply by the continuous relaxation technique. The solution to problem (P3-M) can be fractional if relaxation technique is applied. In this case, it is possible to round down the fractional solution to get a feasible solution by setting $a_\ell^k = \lfloor a_\ell^k \rfloor$. Denote λ_i as the optimal dual variable for constraint (11) in the master problem. By solving problem (P3-M), we can obtain λ_i . Subsequently, the optimality condition of obtained results is verified by

$$\sum_{i \in \mathcal{I}} (\lambda_i - \mu_i) \nu_{i,\ell}^k \geq 0, \quad \forall k, \ell. \quad (24)$$

A generation problem should be triggered if (24) does not hold. For EOS k , the generation problem, (P3-G), becomes

$$\begin{aligned} (\text{P3-G}) \quad & \min \sum_{i \in \mathcal{I}} \sum_{\ell \in \mathcal{L}_k} (\lambda_i - \mu_i) \nu_{i,\ell}^k \\ \text{s.t.} \quad & (20). \end{aligned} \quad (25)$$

To solve problem (P3-G), we first give the definition of multi-constrained optimal path (MCOP) problem [38].

Definition 2. Consider an edge-weighted directed graph $\mathcal{G}_k^{\text{ADG}} = (\mathcal{V}_k^{\text{ADG}}, \mathcal{E}_k^{\text{ADG}})$, with a primary cost parameter $\beta(e)$, and Q additional non-negative real-valued weights $\omega_q(e)$, $1 \leq q \leq Q$, associated with each edge $e \in \mathcal{E}_k^{\text{ADG}}$, a constraint vector $W = (W_1, \dots, W_Q)$ where each W_q is a positive constant, and a source-destination node pair (v_s, v_d) . A MCOP problem is to find a path, π , from v_s to v_d such that $c(\pi) = \sum_{e \in \pi} \beta(e)$ is minimized, subject to the constraints $\omega_q(\pi) = \sum_{e \in \pi} \omega_q(e) \leq W_q$, $1 \leq q \leq Q$.

Lemma 4. *Problem (P3-G) can be equivalently reformulated as a MCOP problem.*

Proof: Set $Q = M$ (Recall that M is the number of segments in the extended transmission time sharing graph). By properly associating each edge, $e \in \mathcal{E}_k^{\text{ADG}}$, with cost $\beta(e)$ and M weights $\omega_q(e)$, $1 \leq q \leq M$, problem P3-G can be transformed into a MCOP problem. As for the cost, if $e = (o_i, o_j)$, we set $\beta(e) = (\lambda_j - \mu_j)\nu_{j,\ell}^k$. We also let $\beta(e) = (\lambda_i - \mu_i)\nu_{i,\ell}^k$ for $e = (v_s, o_i)$ and $\beta(e) = 0$ for $e = (o_i, v_d)$. The objective function in problem (P3-G) thus becomes finding a path, π , such that the total cost of the path $\beta(\pi) = \sum_{e \in \pi} c(e)$ is minimized. Besides, each edge, $e = (o_i, o_j)$, is associated with M weights, $\omega_q(e)$, $1 \leq q \leq M$. In terms of $e = (o_i, o_j)$, set $\omega_q(e) = \rho_j \cdot \nu_{j,\ell}^k \cdot r_k^{\text{ob}}$ and $W_q = \sum_{\vartheta=1}^q D_{k,\vartheta}^{\text{tr}} \cdot r_k^{\text{tr}}$ for $q < g_j$, while set $\omega_q(e) = 0$ and $W_q = 0$ for $q \geq g_j$. To this end, constraints $\omega_q(\pi) = \sum_{e \in \pi} \omega_q(e) \leq W_q$ for $1 \leq q \leq M$ are equivalent to (20). This completes the proof. ■

According to Lemma 4, we can use existing pseudo-polynomial time approximation algorithms [39], [40] to solve problem (P3-G). After solving the overall observation scheduling sub-problem, we can obtain a set of observation sequences $\mathcal{L}^{\text{new}} = \{\ell_1, \ell_2, \dots, \ell_K\}$, with ℓ_k corresponding to the observation sequence for EOS k . Denote $D_{k,m}^{\text{ob}}$ as the required transmission time in segment S_m for delivering all the observation data if ℓ_k is selected for EOS k , given by

$$D_{k,m}^{\text{ob}} = \frac{r_k^{\text{ob}}}{r_k^{\text{tr}}} \sum_{i \in \mathcal{I}_m} \rho_i \quad (26)$$

where \mathcal{I}_m represents the subset of tasks transmitted in segment S_m . Accordingly, the total required transmission time D_k^{ob} for EOS k is expressed as $D_k^{\text{ob}} = \sum_m D_{k,m}^{\text{ob}}$.

C. Redistribution of Surplus Transmission Time

In each iteration, a set of observation sequences $\mathcal{L}^{\text{new}} = \{\ell_1, \ell_2, \dots, \ell_K\}$ is generated. Based on the result, we need to re-adjust the pre-allocated transmission time to match the required transmission time. Specifically, the total remaining transmission time for EOS k is $\max\{0, D_k^{\text{tr}} - D_k^{\text{ob}}\}$. Denote $\mathcal{K}_m^{\text{tr}}$ as the set of EOSs that possess surplus transmission time over segment S_m , i.e., $\max\{0, D_{k,m}^{\text{tr}} - D_{k,m}^{\text{ob}}\} > 0$, $k \in \mathcal{K}_m^{\text{tr}}$. Similarly, the total required transmission time for EOS k is $\max\{0, D_k^{\text{ob}} - D_k^{\text{tr}}\}$. Denote $\mathcal{K}_m^{\text{ob}}$ as the set of EOSs that need more transmission time over segment S_m , i.e., $\max\{0, D_{k,m}^{\text{ob}} - D_{k,m}^{\text{tr}}\} > 0$, $k \in \mathcal{K}_m^{\text{ob}}$. For each EOS, $k \in \mathcal{K}_m^{\text{tr}}$, the surplus transmission time $(D_{k,m}^{\text{tr}} - D_{k,m}^{\text{ob}})$ over segment S_m is equally distributed to a subset of EOSs $\mathcal{K}_m^{\text{ob}}$ that requires transmission time in the segment. We set $D_{k,m}^{\text{tr}} - D_{k,m}^{\text{ob}} = 0$ for EOS $k \in \mathcal{K}_m^{\text{tr}}$ if all its surplus transmission time in S_m is distributed, or there are no EOSs need additional transmission time. The available transmission time for EOS $k \in \mathcal{K}_m^{\text{ob}}$ over segment S_m is updated via

$$D_{k,m}^{\text{tr}} \leftarrow D_{k,m}^{\text{tr}} + \sum_{l \in \mathcal{K}_m^{\text{tr}}} \frac{D_{l,m}^{\text{tr}} - D_{l,m}^{\text{ob}}}{|\mathcal{K}_m^{\text{ob}}|}, \quad \forall k, m. \quad (27)$$

Then, the next iteration starts. The iteration process terminates until $\max\{0, D_k^{\text{tr}} - D_k^{\text{ob}}\} = 0$ holds for all $k \in \mathcal{K}$.

D. Algorithm Description and Analysis

By summarizing the preceding descriptions, the detailed procedure of AMRS algorithm is given in Algorithm 1. First, the algorithm initializes the iteration counter h , successfully scheduled task set \mathcal{I}^* , observation sequence set \mathcal{L}^* , and transmission time vector D^* . An initial extended time sharing graph is built as stated in Subsection IV-A. A small feasible set \mathcal{L}_0 of K observation sequences is chosen for problem (P3). For instance, \mathcal{L}_0 can be constructed by simply assigning a target to the EOS that has the earliest OW for it without violating constraint (20). Second, the transmission scheduling process starts when needed. Surplus transmission time is distributed from EOS $k^* \in \mathcal{K}_m^{\text{tr}}$ to EOS $k \in \mathcal{K}_m^{\text{ob}}$. Third, given an allocated transmission time vector, observation scheduling is done for the set of unscheduled EOSs utilizing state-of-the-art MCOP routing solutions, e.g., [40]. Finally, the iteration continues until all EOSs have no more remaining transmission time.

Algorithm 1 Approximate Multi-Resource Schedule (AMRS)

```

1: // Initialization: Set  $h = 1$ ,  $\mathcal{I}^* = \tilde{\mathcal{A}}\tilde{\mathcal{Y}}$ ,  $\mathcal{L}^* = \tilde{\mathcal{A}}\tilde{\mathcal{Y}}$ , and  $D^* = \mathbf{0}$ . Initiate a small set of observation sequences  $\mathcal{L}_0$  and set  $\mathcal{L}^{\text{new}} = \mathcal{L}_0$ .
2: repeat
3:   // Transmission scheduling:
4:   if  $h = 1$  then
5:     Construct an initial extended time sharing graph and compute  $(D_{1,1}^{\text{tr}}, D_{1,2}^{\text{tr}}, \dots, D_{K,M}^{\text{tr}})$ .
6:   else
7:     // Redistribution of surplus transmission time
8:     Equally distribute the surplus transmission time  $D_{k^*,m}^{\text{tr}} - D_{k^*,m}^{\text{ob}}$  from EOS  $k^* \in \mathcal{K}_m^{\text{tr}}$  to corresponding subset of EOSs, i.e.,  $\mathcal{K}_m^{\text{ob}}$ ;
9:     Add  $D_{k^*,m}^{\text{ob}}$  into  $D^*$ , and set  $D_{k^*,m}^{\text{tr}} - D_{k^*,m}^{\text{ob}} = 0$ ;
10:    For EOS  $k \in \mathcal{K}_m^{\text{ob}}$ , update  $D_{k,m}^{\text{tr}}$  using (27);
11:   end if
12:   // Observation scheduling:
13:   Find a set of observation sequences  $\mathcal{L}^{\text{new}}$  in the constructed ADG by employing MCOP solutions;
14:    $\mathcal{L} \leftarrow (\mathcal{L} \cup \mathcal{L}^{\text{new}}) \setminus \mathcal{L}_{k^*}$ ;
15:    $\mathcal{L}^* \leftarrow \mathcal{L}^* \cup \{\ell_{k^*}\}$ ,  $\mathcal{I}^* \leftarrow \mathcal{I}^* \cup \{i | i \in \ell_{k^*}\}$ ;
16:    $h = h + 1$ ;
17: until  $\max\{0, D_k^{\text{tr}} - D_k^{\text{ob}}\} = 0$  holds for  $\forall k \in \mathcal{K}$ ;
18: Return coordinate scheduling results  $\mathcal{L}^*$  and  $D^*$ .
```

Herein, we analyze the proposed AMRS algorithm in terms of its convergence and computational complexity.

Theorem 1. The AMRS algorithm will eventually terminate.

Proof: In an iteration, if every EOS, $k \in \mathcal{K}$, satisfies $\max\{0, D_k^{\text{tr}} - D_k^{\text{ob}}\} > 0$, we naturally set $\max\{0, D_k^{\text{tr}} - D_k^{\text{ob}}\} = 0$ in the end of the iteration, since no EOS needs additional transmission time. Therefore, the algorithm terminates. Otherwise, there must exist a subset of EOSs, e.g., $k^* \in \mathcal{K}_m^{\text{tr}}$, whose $\max\{0, D_{k^*,m}^{\text{tr}} - D_{k^*,m}^{\text{ob}}\} > 0$. In this case, remaining transmission time in EOS k^* over segment S_m will be reallocated to the subset of EOSs, i.e., $\mathcal{K}_m^{\text{ob}}$, that need it. Thus, after distributing the surplus transmission time from EOS k^* to others, we

have $\max\{0, D_{k^*}^r - D_{k^*}^{ob}\} = 0$. As a result, in each iteration, there is at least one EOS k^* whose $D_{k^*}^r$ becomes zero. By extension, it takes at most K iterations for all EOSs to reach $\max\{0, D_{k^*}^r - D_{k^*}^{ob}\} = 0$, where the algorithm terminates. Hence, theorem 1 is proved. ■

Theorem 2. *The AMRS algorithm has a computational complexity of $O(K^3I^3 + K^3M)$.*

Proof: The complexity of the AMRS algorithm consists of three main parts: 1) transmission scheduling subproblem with the complexity of $O(KN)$ — This complexity comes from building an extended transmission time sharing graph. It takes $O(KN)$ to construct the graph for a SIN with K EOSs and N destinations; 2) observation scheduling subproblem with the complexity of $O(K^2I^3)$ — It corresponds to complexity of master problem $O(K^2)$ and complexity of generation problem $O(I^3)$. For the master problem, an algorithm with $O(K^2)$ complexity can be employed to solve the relaxed linear programming [13]. As for the generation problem, it first takes complexity of $O(I^2)$ to construct an ADG. Then, existing approximation algorithms with complexity of $O(I^3)$ can be devised to solve the equivalent MCOP problem on the ADG [39]. Therefore, the overall computational complexity of generation problem is $O(I^2) + O(I^3) = O(I^3)$; and 3) redistribution of surplus transmission time with complexity of $O(K^2M)$ — In the worst case, for each EOS, its surplus transmission time over M segments are distributed to all other $K - 1$ EOSs. This incurs a complexity of $O(K^2M)$.

The algorithm runs iteratively to obtain the desired solution. It can be seen that at most K iterations can take place. Within each iteration, the complexity is computed as $O(KN) + O(K^2I^3) + O(K^2M) \approx O(K^2I^3 + K^2M)$. We neglect the term $O(KN)$ as the number of targets I is generally much larger than that of destinations N . As a result, the total complexity of the proposed AMRS algorithm is approximately $K \cdot O(K^2I^3 + K^2M)$, namely $O(K^3I^3 + K^3M)$. ■

V. PERFORMANCE EVALUATION

In this section, extensive simulation results are presented to evaluate the performance of our proposed AMRS algorithm. We quantitatively compare it with two baseline algorithms, namely separate scheduling (SS) algorithm and heuristic coordinate scheduling (HCS) algorithm. The two baseline algorithms are derived by combining existing observation scheduling algorithms with an initial transmission scheduling algorithm. In SS algorithm, the observation scheduling problem is solved via the tabu search meta-heuristic [33], while the overlapping segment of transmission resources is equally allocated to corresponding EOSs. While in HCS algorithm, the overlapping part of conflicting TWs is first shared equally among its components. This constraint is then imposed to observation scheduling, which is further solved via the MCOP algorithm embedded in AMRS algorithm [40]. We evaluate the system performance by the following two widely-used metrics in the literature [14]–[16]. The first is sum priorities of all successfully scheduled tasks. The other is guarantee ratio defined as (total number of successfully scheduled tasks / total number of tasks) $\times 100\%$.

Table I
SETTINGS OF A SMALL-SCALE SIN WITH 5 TASKS.

Task No.	Priority	Observation Duration (Slots)
1	5	1
2	8	3
3	4	3
4	6	2
5	3	2

Table II
SCHEDULING RESULTS OF DIFFERENT ALGORITHMS.

Algorithm	Scheduled Task No.	Guarantee Ratio	Sum Priority
SS	1,4,5	60%	14
HCS	1,2,3	60%	17
AMRS	1,2,4,5	80%	22
Optimal	1,2,4,5	80%	22

We conduct experiments in an SIN environment where the targets are randomly spread on the Earth surface with latitude between 0°N and 60°N and longitude between 30°E and 90°E . A number of targets are chosen, and the priority of a target is an integer randomly distributed in the interval $[1, 10]$. The observation time duration of a task randomly takes a value from the set $\{1, 2, 3\}$ time slots. The length of a time slot is set to 1 minute. A number of EOSs are uniformly distributed over 2 sun-synchronous orbits at a height of 619.6km and with inclination 97.86° . We set two relay satellites d_1 and d_2 which lie at nominal longitudes of 176.76°E and 16.65°E as the destinations. The data collection rate and the transmission rate for all EOSs are 300Mb/s. The set of available OWs and TWs are obtained using the Satellite Tool Kit (STK). All the simulations are coded in Matlab simulator.

We present the simulation results from two aspects. For small-scale SINs, we evaluate the optimality gap between AMRS algorithm and the optimal one in terms of sum priorities and guarantee ratio. For large-scale SINs, we compare the two performance metrics of AMRS algorithm with SS and HCS algorithms, and show the impacts of different network parameters (i.e., target number and delay requirement).

A. Optimality Gap Evaluation in a Small-Scale SIN

We first use a small-scale SIN to demonstrate the feasibility and correctness of the developed AMRS algorithm. In the tested SIN, the optimal solution to the ILP optimization problem (P1) can be efficiently obtained using an off-the-shelf solver (e.g., LINGO solver). There are 2 EOSs and a destination d_1 in the small-scale SIN. The considered time horizon has 10 time slots. The number of targets is 5-10 with a step of 1. All targets arrive at the beginning of the time horizon. We do not impose delay requirements, i.e., expected finish times, for all tasks in this case.

An instance for a SIN with 5 targets is given. Targets 1, 2, 3 and 4 can be observed by EOS 1, while targets 1, 3, 4 and 5 can be observed by EOS 2. In addition, target 3 and target 4 are conflicting with each other in both EOSs. The priority and required observation time duration are given in Table I. The maximum available transmission time for EOS 1 and EOS 2 to the destination are 5 and 6 time slots, respectively, among

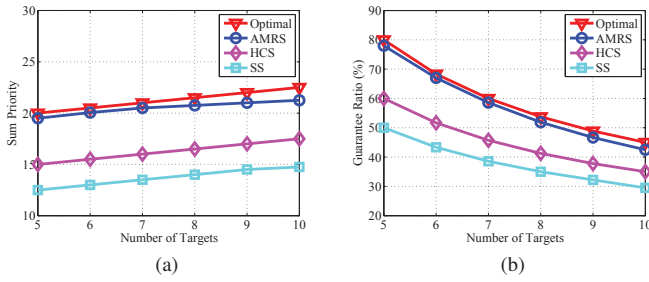


Figure 4. Evaluation of optimality gap in a small-scale SIN.

which 3 time slots can be shared by both EOSs. Table II shows the scheduling results for four different algorithms. In AMRS algorithm, 4 out of 5 tasks can be successfully scheduled. It can be seen that our proposed AMRS algorithm produces the best results in the tested small-scale SIN. Using SS and HCS algorithms, only 3 tasks can be completed. Thus, the guarantee ratio and sum priority performance of SS and HCS algorithms is lower than those of AMRS algorithm.

Fig. 4(a) and 4(b) depict the sum priority and guarantee ratio of different algorithms with varying number of targets in the small-scale SIN. It is observed that AMRS algorithm can achieve a network performance close to that of the optimal solution. We attribute the result to the balanced matching between observation and transmission resources in AMRS algorithm, which boosts the resource utilization. In parallel, SS algorithm performs worst in terms of both the sum priority and guarantee ratio. This is accounted by the imbalance between observation and transmission resources in SS algorithm. Specifically, an EOS scheduled to observe a large number of targets does not receive sufficient transmission time. Consequently, as verified in Fig. 4(b), only a small number of tasks can be completed. In HCS algorithm, the observation decisions are made based on the pre-allocated transmission resources. Since the transmission distribution scheme is sub-optimal, HCS algorithm yields lower network performance as compared with that of AMRS algorithm.

B. Network Performance in a Large-Scale SIN

We consider a large-scale SIN scenario to investigate the effects of different parameters on network performance. Six EOSs and two destinations d_1 and d_2 are deployed in the tested SIN. The time horizon is two hours from 10 Jun 2017 04:00:00 to 10 Jun 2017 06:00:00.

1) *Performance impact of task number*: In this experiment, we investigate the performance impact of the number of tasks that increases from 100 to 200 with an increment step size of 20. The delay requirements of all tasks are set to 120 minutes.

Fig. 5 demonstrates that the sum priority of the three algorithms gradually goes up with the increasing number of targets, because more high priority targets are accepted by exploiting the priority diversity. However, when the number of targets grows large enough, the sum priority does not improve any more. The reason lies in that transmission resources become the bottleneck in this case and additional observation data cannot be downloaded. Fig. 5(b) shows that with an increase of the number of targets, the guarantee ratio of all

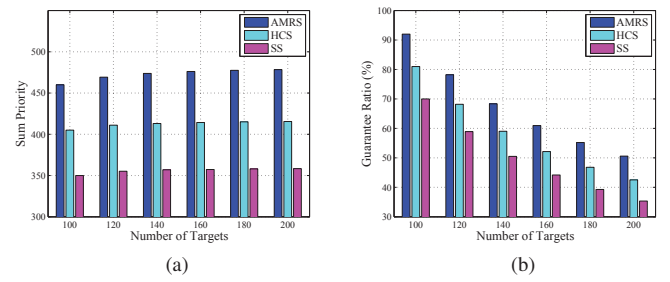


Figure 5. Network performance versus the number of targets.

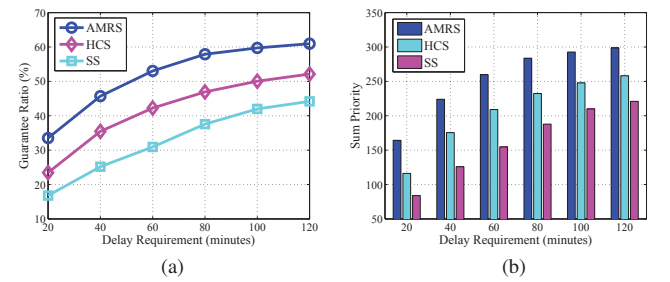


Figure 6. Network performance versus delay requirements.

the three algorithms decreases. This trend is expected, because given the limited resources, increasing the number of targets makes the tested system more heavily loaded, which in turn reduces the guarantee ratio.

2) *Performance impact of delay requirement*: Now we investigate the impact of the delay requirements on the performance of the three algorithms. A batch of 160 tasks arrive at the beginning of the time horizon. The delay requirement of a task varies from 20 to 120 minutes with an increment of 20 minutes. The simulation results are plotted in Fig. 6.

Fig. 6(a) demonstrates that the sum priority of the three algorithms increases with the increase of required delay bound. As the delay requirements of tasks become loose, the available observation and transmission opportunities for tasks increases. More observation data can be stored onboard to reduce the transmission conflicts among multiple EOSs. Consequently, as in Fig. 6(b), more tasks can be accommodated, and the guarantee ratio is improved. This further leads to an increase in the obtained sum priorities. Another observation is that AMRS algorithm achieves superior performance with respect to sum priority and guarantee ratio, in comparison with SS and HCS algorithms. This is because the proposed AMRS algorithm utilizes diverse service requirements of different tasks when making scheduling decisions, while both SS and HCS algorithms neglect the delay requirements. Subsequently, some tasks being scheduled cannot meet their deadlines, and the allocated observation and transmission resources for the tasks are wasted.

VI. CONCLUSIONS AND FUTURE WORK

In this paper, we investigate the problem of multi-resource coordinate scheduling for SINs. Based on an iterative optimization method, a low complexity joint scheduling algorithm, i.e., the AMRS algorithm, is proposed to properly balance the observation and transmission resources. As a result, each

EOS can effectively observe a subset of targets according to its available transmission resources. Extensive simulations have been conducted to verify that the newly proposed AMRS algorithm performs close to the optimal solution in the tested small-scale SINS. In large-scale SINS, AMRS algorithm is shown to outperform two benchmark algorithms in terms of both the sum priority and guarantee ratio.

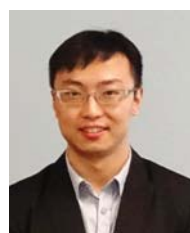
There are a few open issues to be addressed for future studies. First, we intend to take time-varying capacity of both the observation and transmission resources into consideration. Second, we will extend the SIN scenario considered in this paper to include high altitude platforms (HAPs) as essential counterparts. Finally, we plan to develop new scheduling algorithms for dynamic observation tasks whose arrival times are not known in advance.

REFERENCES

- [1] M. Sheng, Y. Wang, J. Li, R. Liu, D. Zhou, and L. He, "Toward a flexible and reconfigurable broadband satellite network: resource management architecture and strategies," *IEEE Wireless Commun.*, vol. 24, no. 4, pp. 127–133, Jun. 2017.
- [2] H. Ramapriyan, "The role and evolution of NASA's earth science data systems," <http://ntrs.nasa.gov>, 2015.
- [3] G. Wu, W. Pedrycz, H. Li, M. Ma, and J. Liu, "Coordinated planning of heterogeneous earth observation resources," *IEEE Trans. Syst., Man, Cybern. Syst.*, vol. 46, no. 1, pp. 109–124, Jan. 2016.
- [4] C. Jiang, X. Wang, J. Wang, H.-H. Chen, and Y. Ren, "Security in space information networks," *IEEE Commun. Mag.*, vol. 53, no. 8, pp. 82–88, Aug. 2015.
- [5] Q. Yu, W. Meng, M. Yang, L. Zheng, and Z. Zhang, "Virtual multi-beamforming for distributed satellite clusters in space information networks," *IEEE Wireless Commun.*, vol. 23, no. 1, pp. 95–101, Feb. 2016.
- [6] J. Du, C. Jiang, Y. Qian, Z. Han, and Y. Ren, "Resource allocation with video traffic prediction in cloud-based space systems," *IEEE Trans. Multimedia*, vol. 18, no. 5, pp. 820–830, May 2016.
- [7] J. A. Fraire and J. M. Finochietto, "Design challenges in contact plans for disruption-tolerant satellite networks," *IEEE Commun. Mag.*, vol. 53, no. 5, pp. 163–169, May 2015.
- [8] Z. Zhou, M. Dong, Z. Chang, and B. Gu, "Combined centralized and distributed resource allocation for green D2D communications," in *Proc. IEEE/CIC ICC*, Nov. 2015, pp. 1–6.
- [9] Q. Ye and W. Zhuang, "Token-based adaptive MAC for a two-hop internet-of-things enabled MANET," *IEEE Internet of Things Journal*, vol. 4, no. 5, pp. 1739–1753, Oct. 2017.
- [10] S. Zhang, N. Zhang, S. Zhou, J. Gong, Z. Niu, and X. Shen, "Energy-aware traffic offloading for green heterogeneous networks," *IEEE J. Sel. Areas Commun.*, vol. 34, no. 5, pp. 1116–1129, May 2016.
- [11] W. J. Wolfe and S. E. Sorensen, "Three scheduling algorithms applied to the earth observing systems domain," *Management Science*, vol. 46, no. 1, pp. 148–168, Jan. 2000.
- [12] D. Y. Liao and Y. T. Yang, "Imaging order scheduling of an earth observation satellite," *IEEE Trans. Syst., Man, Cybern. C, Appl. Rev.*, vol. 37, no. 5, pp. 794–802, Sep. 2007.
- [13] Z. Zhang, C. Jiang, S. Guo, Z. Ni, and Y. Ren, "Optimal satellite scheduling with critical node analysis," in *Proc. IEEE WCNC*, San Francisco, CA, USA, 2017, pp. 1–6.
- [14] J. Wang, X. Zhu, D. Qiu, and L. T. Yang, "Dynamic scheduling for emergency tasks on distributed imaging satellites with task merging," *IEEE Trans. Parallel Distrib. Syst.*, vol. 25, no. 9, pp. 2275–2285, Jun. 2014.
- [15] X. Zhu, J. Wang, X. Qin, J. Wang, Z. Liu, and E. Demeulemeester, "Fault-tolerant scheduling for real-time tasks on multiple earth-observation satellites," *IEEE Trans. Parallel Distrib. Syst.*, vol. 26, no. 11, pp. 3012–3026, Nov. 2015.
- [16] X. Zhu, K. M. Sim, J. Jiang, J. Wang, C. Chen, and Z. Liu, "Agent-based dynamic scheduling for earth-observing tasks on multiple airships in emergency," *IEEE Syst. Journal*, vol. 10, no. 2, pp. 661–672, Jun. 2016.
- [17] J. A. Fraire, P. G. Madoery, and J. M. Finochietto, "On the design and analysis of fair contact plans in predictable delay-tolerant networks," *IEEE Sensors Journal*, vol. 14, no. 11, pp. 3874–3882, Nov. 2014.
- [18] J. Fraire, P. Madoery, and J. Finochietto, "Routing aware fair contact plan design for predictable delay tolerant networks," *Elsevier Ad-Hoc Networks*, vol. 25, pp. 303–313, Feb. 2015.
- [19] K. Kaneko, Y. Kawamoto, H. Nishiyama, N. Kato, and M. Toyoshima, "An efficient utilization of intermittent surface-satellite optical links by using mass storage device embedded in satellites," *Performance Evaluation*, vol. 87, pp. 37–46, May 2015.
- [20] Y. Wang, M. Sheng, J. Li, X. Wang, R. Liu, and D. Zhou, "Dynamic contact plan design in broadband satellite networks with varying contact capacity," *IEEE Commun. Letters*, vol. 20, no. 16, pp. 2410–2413, Dec. 2016.
- [21] X. Jia, T. Lv, F. He, and H. Huang, "Collaborative data downloading by using inter-satellite links in LEO satellite networks," *IEEE Trans. Wireless Commun.*, vol. 16, no. 3, pp. 1523–1532, Mar. 2017.
- [22] B. Deng, C. Jiang, L. Kuang, S. Guo, J. Lu, and S. Zhao, "Two-phase task scheduling in data relay satellite systems," *IEEE Trans. Veh. Technol.*, vol. PP, no. 99, pp. 1–11, Oct. 2017.
- [23] N. Bianchessi and G. Righini, "Planning and scheduling algorithms for the COSMO-SkyMed constellation," *Aerospace Science and Technology*, vol. 12, pp. 535–544, 2008.
- [24] H. Chen, J. Wu, W. Shi, J. Li, and Z. Zhong, "Coordinate scheduling approach for EDS observation tasks and data transmission jobs," *Journal of Systems Engineering and Electronics*, vol. 27, no. 4, pp. 822–835, Aug. 2016.
- [25] R. Liu, M. Sheng, K.-S. Lui, X. Wang, Y. Wang, and D. Zhou, "An analytical framework for resource-limited small satellite networks," *IEEE Commun. Letters*, vol. 20, no. 2, pp. 388–391, Feb. 2016.
- [26] D. Zhou, M. Sheng, X. Wang, C. Xu, R. Liu, and J. Li, "Mission aware contact plan design in resource-limited small satellite networks," *IEEE Trans. Commun.*, vol. 65, no. 6, pp. 2451–2466, Mar. 2017.
- [27] Y. Li, C. Song, D. Jin, and S. Chen, "A dynamic graph optimization framework for multihop device-to-device communication underlying cellular networks," *IEEE Wireless Commun.*, vol. 21, no. 5, pp. 52–61, Oct. 2014.
- [28] F. Malandrino, C. Casetti, C.-F. Chiasserini, and M. Fiore, "Optimal content downloading in vehicular networks," *IEEE Trans. Mobile Comput.*, vol. 12, no. 7, pp. 1377–1391, Jul. 2013.
- [29] V. Gabrel, A. Moulet, C. Murat, and V. T. Paschos, "A new single model and derived algorithms for the satellite shot planning problem using graph theory concepts," *Annals of Operations Research*, vol. 69, pp. 115–134, 1997.
- [30] J. A. Fraire and J. M. Finochietto, "Design challenges in contact plans for disruption-tolerant satellite networks," *IEEE Commun. Mag.*, vol. 53, no. 5, pp. 163–169, May 2015.
- [31] M. Azimifar, T. D. Todd, A. Khezrian, and G. Karakostas, "Vehicle-to-vehicle forwarding in green roadside infrastructure," *IEEE Trans. Veh. Technol.*, vol. 65, no. 2, pp. 780–795, Feb. 2016.
- [32] V. Gabrel, "Strengthened 0-1 linear formulation for the daily satellite mission planning," *J. Combinat. Optim.*, vol. 11, no. 3, pp. 341–346, 2006.
- [33] N. Bianchessi and *et al.*, "A heuristic for the multi-satellite, multi-orbit and multiuser management of earth observation satellites," *Eur. J. Oper. Res.*, vol. 177, no. 2, pp. 750–762, 2007.
- [34] H. Vance, C. Barnhart, E. Johnson, and G. L. Nemhauser, "Solving binary cutting stock problems by column generation and branch-and-bound," *Computational Optimization and Applications*, vol. 3, pp. 111–130, May 1994.
- [35] C. Mancel and P. Lopez, "Complex optimization problems in space systems," in *Proc. 13th International Conf. Automated Planning & Scheduling (ICAPS'03)*, Trento, Italy, Jun. 2003, pp. 1–5.
- [36] B. Chandra and M. M. Halldorsson, "Greedy local improvement and weighted set packing approximation," *Journal of Algorithms*, vol. 39, no. 2, pp. 223–240, May 2001.
- [37] P. Berman, "A d/2 approximation for maximum weight independent set in d-claw free graphs," *Algorithm Theory*, pp. 214–219, Berlin, Germany: Springer, Jul. 2000.
- [38] T. Korkmaz and M. Krunz, "Multi-constrained optimal path selection," in *Proc. IEEE INFOCOM*, 2001, pp. 834–843.
- [39] M. Song and S. Sahni, "Approximation algorithms for multiconstrained quality-of-service routing," *IEEE Trans. Computers*, vol. 55, no. 5, pp. 603–617, May 2006.
- [40] G. Xue, W. Zhang, J. Tang, and K. Thulasiraman, "Polynomial time approximation algorithms for multi-constrained QoS routing," *IEEE/ACM Trans. Netw.*, vol. 16, no. 3, pp. 656–669, Jun. 2008.



Yu Wang received the B.S. degree in telecommunications engineering from Xidian University, Xian, China, where he is currently pursuing his Ph.D. degree in communication and information systems. He is also a visiting Ph.D. student from Aug. 2016 to Aug. 2017 in Department of Electrical and Computer Engineering, University of Waterloo. His research interests include software-defined networking, resource allocation and satellite networks.



Ning Zhang (M'15) received his Ph.D degree from the University of Waterloo in 2015. He is now an assistant professor in the Department of Computing Science at Texas A&M University-Corpus Christi. Before that, he was a postdoctoral research fellow at the University of Waterloo and at the University of Toronto. He is the recipient of the Best Paper Award at IEEE Globecom 2014 and IEEE WCSP 2015. He is a lead guest editor of Wireless Communications and Mobile Computing and International Journal of Distributed Sensor Networks, and a guest editor of Mobile Information System. His current research interests include next generation wireless networks, software defined networking, vehicular networks, and physical layer security.



Min Sheng (M'03-SM'16) received the M.S. and Ph.D. degrees in communication and information systems from Xidian University, Shaanxi, China, in 2000 and 2004, respectively. She has been a faculty member at the School of Telecommunications Engineering at Xidian University since 2000, where she is currently a full professor with the State Key Laboratory of ISN. Her current research interests include interference and resource management in heterogeneous networks, ultra dense networks (UDN), self-organizing networks (SON), big data processing,

green communications, and satellite networks. She has published two books and over 130 papers in refereed journals and conference proceedings. She was honored with the Second Prize for the State Technological Innovation Award in 2014, the New Century Excellent Talents in University by the Ministry of Education of China, the Young Teachers Award from the Fok Ying-Tong Education Foundation, China, in 2008, and the Best Paper Award at IEEE/CIC ICC 2013.



Runzi Liu (M'16) received the B.S. degree in telecommunications engineering at Xidian University, Xi'an, China, where she is currently pursuing the Ph.D. degree in communication and information systems. Her research interests include routing and capacity analysis in ad hoc networks and satellite networks.



Weihua Zhuang (M'93-SM'01-F'08) has been with the Department of Electrical and Computer Engineering, University of Waterloo, Canada, since 1993, where she is a Professor and a Tier I Canada Research Chair in Wireless Communication Networks. She is a co-recipient of several best paper awards from IEEE conferences. Dr. Zhuang was the Editor-in-Chief of IEEE Transactions on Vehicular Technology (2007-2013), Technical Program Chair/Co-Chair of IEEE VTC Fall 2017 and Fall 2016, and the Technical Program Symposia Chair of the IEEE

Globecom 2011. She is a Fellow of the IEEE, the Royal Society of Canada, the Canadian Academy of Engineering, and the Engineering Institute of Canada. Dr. Zhuang is an elected member in the Board of Governors and VP Publications of the IEEE Vehicular Technology Society. She was an IEEE Communications Society Distinguished Lecturer (2008-2011).



Jiandong Li (SM'05) received his B.S., M.S., and Ph.D. degrees in communications and electronic systems from Xidian University in 1982, 1985, and 1991, respectively. In 1985, he joined Xidian University, where he has been a professor since 1994 and the vice-president since 2012. His current research interests and projects consist of mobile communications, broadband wireless systems, ad hoc networks, cognitive and software radio, self-organizing networks, and game theory for wireless networks. He is a Fellow of the China Institute of Electronics and a Fellow of the China Institute of Communication. He was a member of the PCN Specialist Group for the China 863 Communication High Technology Program between January 1993 and October 1994 and from 1999 to 2000. He is also a member of the Communication Specialist Group for the Ministry of Industry and Information.



Shan Zhang (S'13-M'16) received her Ph.D. degree in Department of Electronic Engineering from Tsinghua University and B.S. degree in Department of Information from Beijing Institute Technology, Beijing, China, in 2016 and 2011, respectively. She is currently a post doctoral fellow in Department of Electrical and Computer Engineering, University of Waterloo, Ontario, Canada. Her research interests include resource and traffic management for green communication, intelligent vehicular networking, and software defined networking. Dr. Zhang

received the Best Paper Award at the Asia-Pacific Conference on Communication in 2013.